Enhanced Interfacial Magnetic Coupling of Gd/Fe Multilayers

D. Haskel,[1] G. Srajer,[1] J.C. Lang,[1] J. Pollmann,[1] C.S. Nelson,[1,*] J.S. Jiang,[2] and S.D. Bader[2]

[1]*Advanced Photon Source, Argonne National Laboratory, Argonne, Illinois 60439*

[2]*Materials Science Division, Argonne National Laboratory, Argonne, Illinois 60439*

(Received 2 August 2001; published 24 October 2001)

The spatial extent ζ_{AFM} and strength J_{AFM} of the antiferromagnetic (AFM) exchange coupling at buried Gd/Fe interfaces in ferrimagnetic $[\mathrm{Gd}(50\ \text{Å})\mathrm{Fe}(15,35\ \text{Å})]_{15}$ sputtered multilayers is obtained from combined x-ray resonance magnetic reflectivity and magnetic circular dichroism measurements. ζ_{AFM} is 4.1(7) Å or $\sim 1-2$ interatomic distances in bulk Gd and Fe; J_{AFM} is 1050(90) K, comparable to the ferromagnetic exchange in bulk Fe.

DOI: 10.1103/PhysRevLett.87.207201 PACS numbers: 75.70.–i, 75.25.+z, 75.75.+a

Understanding the nature of magnetic interactions at the interfaces of atomically engineered nanostructures has been the focus of many recent investigations [1–7]. The renewed interest is partly driven by the role interfaces play in magnetic thin-film devices. For example, chemical interfacial roughness affects spin-polarized transport and the giant magnetoresistance effect in magnetic Fe/Cr superlattices and spin valves [2,8]. At a more fundamental level interfacial magnetic disorder accompanying chemical roughness introduces uncompensated spins at ferromagnetic-antiferromagnetic exchange-biased interfaces [9] and affects magnetization reversal processes [10]. While different approaches have been pursued to derive fundamental properties of magnetic interfaces [1,5,7], few quantitative studies on buried magnetic interfaces have been reported to date [4,7,11–13].

The experimental difficulty lies in isolating interfacial from "bulk" regions and separating the contributions of different magnetic species in complex systems. Here we report results from x-ray resonance magnetic reflectivity and x-ray magnetic circular dichroism (XMCD) techniques that allow us to derive interfacial magnetic properties with unprecedented accuracy. The high flux available at third-generation synchrotron sources permits magnetization density profiles to be obtained with higher spatial resolution than presently possible with polarized neutrons [14] (here $q_{z,\max} \approx 0.7\ \text{Å}^{-1}$, $q_z = |\vec{k}_i - \vec{k}_f|$). Resonance enhancement of magnetic contrast in these x-ray techniques [15,16] provides element-specific information and simplifies data interpretation. The high penetrating power of hard x rays, $\sim 1\ \mu$m at the Gd $L_{2,3}$ resonances, results in properties representative of the whole structure.

A key issue of great current interest concerns enhanced magnetic properties at interfaces. Polycrystalline and single crystalline Gd (0001) surfaces are known to exhibit enhanced magnetic order [17] while proximity to nonmagnetic Y reduces the Gd magnetization at Gd/Y interfaces [11]. Here we show that proximity to high Curie temperature (T_c) Fe (1024 K) enhances the magnetization of low-T_c Gd (293 K) at Gd/Fe interfaces. Magnetic resonance reflectivity shows a 4.1(7) Å Gd interfacial region near Fe which remains fully magnetized above its bulk T_c value giving a measure of the spatial extent of the interlayer exchange coupling. The size of this interfacial region was confirmed by temperature-dependent XMCD which also yields an elevated T_c of $\approx$1050(90) K for the interfacial region.

The multilayers were sputtered in vacuum onto Si substrates using Nb buffer (100 Å) and cap (30 Å) layers. SQUID magnetometry suggests, and the x-ray measurements confirm, that in the Gd(50 Å)/Fe(15 Å) multilayer the Gd magnetization is parallel to the applied field while that of Fe is antiparallel up to at least 350 K. Since Gd and Fe have similar bulk saturation magnetization values M_0 (2020 and 1750 emu/cm^3, respectively), this configuration is expected at low temperatures due to the larger Zeeman energy $-\vec{M}_0 \cdot \vec{B}$ contribution of the thicker Gd layer. What is surprising is that Gd dominates the Zeeman energy even above the Gd bulk T_c of 293 K. The Gd(50 Å)/Fe(35 Å) multilayer has a compensation temperature of 135 K, where the Fe magnetization aligns with the field, Gd antiparallel. Our results quantitatively explain the different behaviors of these multilayers.

X-ray measurements were performed at Sector 4 of the Advanced Photon Source at Argonne National Laboratory. Undulator radiation was monochromatized with double Si(111) crystals and its polarization converted from linear to circular with a diamond (111) quarter-wave plate operated in Bragg transmission geometry [18]. The sample was placed in a $B = 2.1$ kG field parallel to its surface and in the scattering plane (coercive field is $\lesssim$100 G). The sample and magnet were placed inside a closed-cycle He refrigerator mounted in the ϕ circle of a diffractometer. Specular magnetic reflectivity was measured with a photon energy near the Gd L_2 resonance (7929 eV) across six multilayer Bragg peaks by switching the helicity of the incident radiation at each scattering vector $q_z = (4\pi/\lambda)\sin\theta$, with θ being the grazing incidence angle. XMCD was measured in fluorescence in a 100 eV energy range around the Gd $L_{2,3}$ absorption edges.

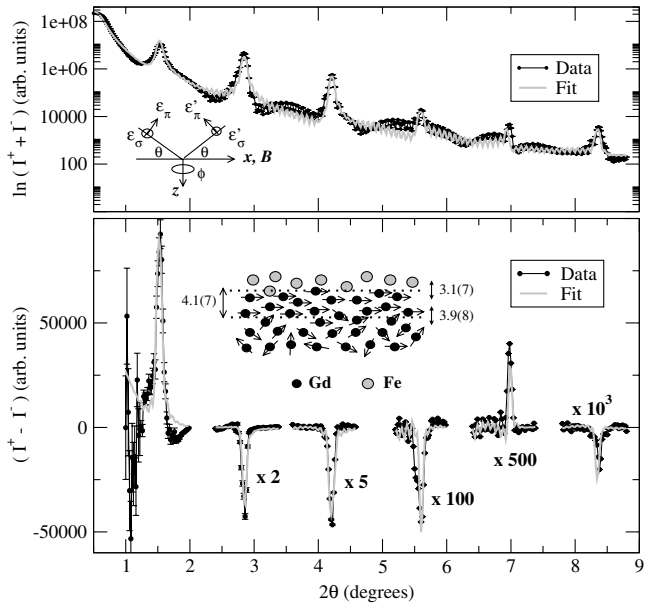

FIG. 1. Charge (top) and charge-magnetic interference (bottom) specular reflectivity (points) and fits (lines) for $E = 7929$ eV and 300 K. The top inset shows scattering geometry and applied field direction with θ being the incident angle and $\hat{\epsilon}$, $\hat{\epsilon}'$ polarization vectors of incident and scattered radiation, respectively (shown in σ, π representation). The bottom inset shows a derived interfacial magnetic structure indicating the extent of the magnetized interfacial region [4.1(7) Å] and values of charge and magnetic roughness of Gd/Fe [3.1(7) Å] and Gd ferromagnetic-paramagnetic [3.9(8) Å] interfaces.

Figure 1 shows specular reflectivity curves for the Gd(50 Å)/Fe(15 Å) multilayer as obtained by adding (top) and subtracting (bottom) scattered intensities for opposite helicities of the incoming radiation. While the sum reflectivity relates to interference between waves scattered from charge density variations, the difference reflectivity results from interference between waves scattered from both charge *and* magnetic density variations, as explained below.

To model this interference we used the first Born approximation which assumes weak scattering and is valid away from the regime of total reflection. This approximation has been applied extensively in studies of layered systems with rough interfaces [19]. We focus on the cross section for magnetic reflectivity using circularly polarized x rays as applied to a system with a variable number of interfaces with both charge and magnetic roughness. Following Hannon *et al.* [15], the coherent elastic scattering length of a single magnetic ion in the electric dipole approximation is

$$f = (f_0 + f_e)(\hat{\epsilon}'^* \cdot \hat{\epsilon}) + i f_m (\hat{\epsilon}'^* \times \hat{\epsilon}) \cdot \hat{m}\,, \qquad (1)$$

where we neglect the smaller terms responsible for linear dichroism and nonresonant magnetic scattering. Here $f_0 = -Zr_0$, f_e and f_m are anomalous charge and magnetic scattering lengths, $\hat{\epsilon}$ and $\hat{\epsilon}'$ are polarization vectors of the incoming and scattered radiation, respectively, and $\hat{m}$ is the local moment direction. f_e includes contributions from resonant ($2p_{1/2} \rightarrow 5d$) as well as from transitions involving lower energy absorption edges. f_m is most significant near resonance; it is the difference in scattering lengths for right- and left-circularly polarized x rays whose imaginary part is responsible for the circular dichroism. The strong energy dependence of f_e and f_m near resonance, which includes band structure and core-hole effects, requires that they be determined experimentally on the sample under study.

The scattering amplitude obtained from squaring Eq. (1) includes pure charge and magnetic terms and charge-magnetic cross terms. Pure charge and magnetic terms are independent of x-ray helicity, the latter depending on the square of the magnetization direction (reversing magnetization direction is equivalent to reversing helicity). The *difference* cross section measured in magnetic reflectivity then includes contributions from only the charge-magnetic cross terms. Neglecting internal atomic structure ($q_z^{-1} \gg$ interatomic distance) this cross section in the first Born approximation involves products of the charge and magnetic density contrasts at the interfaces, integrated over the charge and magnetic scattering volumes.

By evaluating the volume integrals by perturbing the interfaces with charge and magnetic roughness [19–21], we obtain, for a system of N interfaces,

$$\Delta \frac{d\sigma}{d\Omega} = \frac{4\pi^2 L_x L_y \delta(q_x)\delta(q_y)}{q_z^2} [\cos 2\theta (\hat{k}_i \cdot \hat{m}) + (\hat{k}_f \cdot \hat{m})] \times \sum_{i,j}^{N} e^{iq_z(z_i - z_j)} [\Delta\rho_{e,i}^* \Delta\rho_{m,j} e^{-q_z^2(\sigma_{e,i}^2 + \sigma_{m,j}^2)/2} + \Delta\rho_{e,j} \Delta\rho_{m,i}^* e^{-q_z^2(\sigma_{e,j}^2 + \sigma_{m,i}^2)/2}], \qquad (2)$$

where $\Delta\rho_{e,i}^* = [n_e^{i+1}(f_0 + f_e^*)^{i+1} - n_e^i (f_0 + f_e^*)^i]$ and $\Delta\rho_{m,j} = (n_e^{j+1} f_m^{j+1} - n_e^j f_m^j)$, i.e., the charge and magnetic density contrasts across interfaces i, j, respectively (n_e is the atomic number density, and $\hat{k}_{i,f}$ are the wave vectors of the incident and scattered radiation). Here $\langle [\delta z_{e,m}(x,y)]^2 \rangle = \sigma_{e,m}^2$ are mean squares of height fluctuations, assumed Gaussian, about the average positions of the charge and magnetic interfaces. The polarization factor in Eq. (2) was calculated for our scattering geometry (Fig. 1) in the (σ, π) representation using the matrix formalism of Blume and Gibbs [22]. This involves taking traces over matrix products of the form $\langle \hat{\epsilon}'^* \cdot \hat{\epsilon} \rangle \rho \langle [(\epsilon'^* \times \hat{\epsilon}) \cdot \hat{m}]^* \rangle$, where ρ is the (2×2) density matrix of a circularly polarized incident beam.

Since we only discuss collinear magnetic structures, the polarization factor involving the local magnetization direction is constant across the Gd-layer thickness. The magnitude of the local magnetization is allowed to vary through

the resonant f_m's. The cross section in Eq. (2) is sensitive only to the magnetization density in the scattering plane. We confirmed the collinear nature of the magnetization by using a $\phi = 90°$ scattering geometry (applied field perpendicular to the scattering plane; Fig. 1), which causes the difference signal to vanish. For simplicity Eq. (2) has $e^{iq_z(z_i - z_j)}$ for the phase difference of the i, j interfaces but phase retardation and absorption effects are included in the fits [23].

Quantitative analysis requires accurate values of the complex charge and magnetic anomalous scattering factors, $f_{e,m} = f'_{e,m} + if''_{e,m}$, at the resonant energy. Through the optical theorem, $f''_{e,m}(E) \propto (E/r_0 n_e hc) \times \mu_{e,m}(E)$ with $\mu_{e,m}$ being the charge and magnetic absorption coefficients. We measured the energy dependence of the absorption coefficient for opposite helicities, $\mu^{\pm}(E)$, in a 100-eV interval around the Gd L_2 edge at 16 K to obtain edge-step normalized $f''_{e,m}$ ($\mu_e = [\mu^+ + \mu^-]/2$, $\mu_m = \mu^+ - \mu^-$) and used tabulated bare-atom scattering factors *away* from resonance for absolute normalization. Real parts were obtained from differential Kramers-Kronig transforms of imaginary parts. At 7929 eV (1 eV below the first inflection point in the absorption coefficient of a Gd foil) these factors are $f_e = -17.3 + 13.4i$ and $f_m = 0.22 - 0.26i$.

The charge ($I^+ + I^-$) specular reflectivity data were analyzed using a Parratt fit [24], modified to include roughness, to extract average layer thicknesses, $t_{\mathrm{Fe}} = 14.73(4)$ Å, $t_{\mathrm{Gd}} = 50.20(4)$ Å; electron densities, $\rho_{\mathrm{Fe}} = 1.97(6)e/\text{Å}^3$, $\rho_{\mathrm{Gd}} = 1.82(5)e/\text{Å}^3$; and rms interfacial roughness, $\sigma_e(\mathrm{Gd/Fe}) = 3.1(7)$ Å (Fig. 1, top panel). Fitted electron densities are ~5%–10% reduced from their bulk values. Fits to the charge-magnetic ($I^+ - I^-$) specular reflectivity data were carried out by describing the magnetization profile in Gd layers with an interfacial region near Fe with adjustable thickness and magnetization and a bulklike region whose magnetization exponentially decays, with adjustable decay rate, from its value at the interfacial region. Adjustable interfacial magnetic roughnesses were used at the Gd/Fe and Gd/Gd interfaces, the latter constrained to be the same. These five adjustable parameters are refined in a nonlinear least-squares fit to the data following Eq. (2) with measured $f_{e,m}$ scattering factors. Uncertainties are obtained by inverting the curvature matrix of a χ^2 statistic and include correlations between fitting parameters. The value of f_m at 16 K determines the absolute scale for a saturated Gd magnetization which is nearly identical to that of a saturated Gd foil, as seen by the same $\mu_m(E)/\mu_e(E)$ ratios [maximum contrast 5.0(2)%].

Best fits at 16 K show that the Gd layer is nearly fully magnetized, the average magnetization over the layer thickness $\gtrsim$94% of its saturation value. This justifies using f_m determined from the 16 K dichroism measurement, an average over the Gd layer thickness, as the absolute scale for a saturated magnetization. At 300 K, i.e., above the bulk T_c of Gd, best fits indicate that the Gd layer is paramagnetic, except for a 4.1(7) Å thick region that remains fully magnetized near the Gd/Fe interface (Fig. 1, bottom panel). This magnetization is induced by a strong antiferromagnetic (AFM) exchange interaction with the magnetically ordered Fe layers, as predicted in mean-field calculations by Camley [25]. The size of this region is a measure of the spatial extent of this AFM interaction. This extent is intrinsic to the Gd/Fe interface, as the same value (within uncertainties) is obtained at 300 K for the Gd(50 Å)/Fe(35 Å) multilayer. Fitted values of magnetic roughness for Gd/Fe and Gd-ferromagnetic/Gd-paramagnetic interfaces are $\sigma_m = 3.5(9)$, 3.9(8) Å, respectively.

Similar charge and magnetic roughnesses at the Gd/Fe and Gd ferromagnetic-paramagnetic interfaces are expected *if* the charge and magnetic roughnesses are correlated. Our observation of *diffuse* resonant charge-magnetic interference scattering on the same multilayers, both for transverse (q_x) and for longitudinal offset ($\approx q_z$) scans, confirms this correlation in height fluctuations at the charge and magnetic interfaces [20,26].

We confirm the presence and size of this ordered Gd region by temperature-dependent XMCD measurements. Figure 2 shows the intensity of the XMCD signal (integrated area) at the Gd L_2 edge of the Gd(50 Å)/Fe(15 Å)

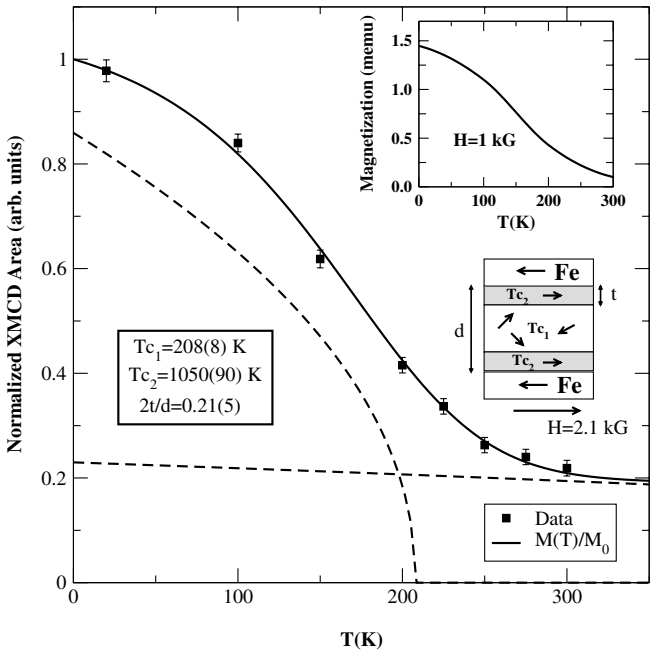

FIG. 2. Integrated XMCD data (points) along with a fit to the data (curve) assuming interfacial and bulklike regions with the same saturation magnetization M_0 but different (varied) T_c values and fractional volumes, $f_v = 2t/d$, $(1 - 2t/d)$, respectively, $M(T)/M_0 = f_v(1 - T/T_c)^{\beta}$; $\beta = 0.47(12)$. The individual fitted components are also shown (dashed curves). The fit to the data includes a convolution with a $\sigma = 12$ K Gaussian to account for disorder in the sputtered layers. The inset shows SQUID magnetization data.

multilayer. At 300 K the Gd layers retain ≈20% of their saturation magnetization, consistent with the magnetic reflectivity result that 17% of the layer remains fully magnetized at 300 K. The same volume fraction (within uncertainties) remains magnetized in a Gd(50 Å)/Fe(35 Å) multilayer at 300 K, but here the Gd XMCD signal has changed sign (relative to 20 K) due to the transition into the Fe-aligned (Gd-antiparallel) configuration at 135 K. By modeling the XMCD intensity as a superposition of interfacial and bulklike regions with adjustable volume fractions and T_c, we find that a $t = 5.2 \pm 1.2$ Å region remains magnetized at 300 K with an estimated $T_c = 1050(90)$ K. Since this magnetized region is induced by the strong AFM exchange interaction at the Gd/Fe interface, its T_c value quantifies the strength of this interaction, $J_{\mathrm{AFM}} \approx J_{\mathrm{Fe}} \approx 1000$ K. An enhanced $T_c \approx 800$ K was previously reported for one monolayer of Gd on an Fe(100) substrate [27]. The $T_c = 208(8)$ K of the bulk region is significantly reduced from that of bulk Gd (293 K). Such a reduction is expected in thin ferromagnetic films [13,28].

The 8–10 Å magnetized regions near Gd/Fe interfaces result in a Gd magnetization that dominates the Zeeman energy even at 300 K in a multilayer with 15 Å Fe thickness. However, based on bulk magnetization values this imbalance is expected to be at its limit, resulting in a near-zero total magnetization (inset of Fig. 2). Increasing the Fe thickness should result in compensation temperatures below 300 K, as observed for a 35 Å Fe multilayer.

XMCD sum rules [29] show no significant enhancement of the Gd $5d$ orbital *and* spin moments in the interfacial regions relative to bulklike regions. At 16 K the XMCD signal is dominated by bulklike Gd regions while at 300 K it arises only from the magnetized interfacial regions. Since sum rules are normalized by the strength of the resonant charge absorption [29], we renormalized the derived moments at 300 K by the fractional magnetized volume found by magnetic reflectivity. Using $n_h = 8.2$ for the $5d$ band-hole occupancy [30] we obtain $\langle L_z \rangle < 7.5 \times 10^{-3} \mu_B$/Gd at 16 and 300 K. Since the Gd $5d$ bands are extended [31], the similar size and shape of XMCD signals in bulklike and interfacial regions suggest similar Gd local environments. The lack of enhancement of $5d$ band polarization at Gd interfacial regions might indicate a more active role for the $6s$ component of the strongly hybridized $(5d, 6\,\mathrm{s})$ band in mediating the indirect exchange between localized $4f$ moments (s-f model [31]), which is stronger at the interface.

In conclusion we extract, with unprecedented accuracy, fundamental parameters characterizing buried magnetic interfaces in Gd/Fe multilayers. The proximity to high-T_c Fe dramatically enhances the Gd magnetization near Gd/Fe interfaces.

We thank S. K. Sinha, D. R. Lee, J. W. Freeland and H. Hashizume for fruitful discussions, M. Newville for error analysis routines, and Y. Choi for experimental help. Work at Argonne is supported by the U.S. DOE, Office of Science, under Contract No. W-31-109-ENG-38.

*Current address: Physics Department, Brookhaven National Laboratory, Upton, New York 11973.

[1] E. Arenholz *et al.,* Phys. Rev. Lett. **80**, 2221 (1998).
[2] R. Schad *et al.,* Europhys. Lett. **44**, 379 (1998).
[3] J. F. Gregg *et al.,* Phys. Rev. Lett. **77**, 1580 (1996).
[4] J. W. Freeland *et al.,* Phys. Rev. B **60**, R9923 (1999).
[5] H. H. Bertschat, J. Magn. Magn. Mater. **198-199**, 636 (1999).
[6] S. Zoll *et al.,* Europhys. Lett. **39**, 323 (1997).
[7] T. Shinjo and W. Keune, J. Magn. Magn. Mater. **200**, 598 (1999).
[8] S. Bae *et al.,* J. Appl. Phys. **87**, 6980 (2000).
[9] K. Takano *et al.,* Phys. Rev. Lett. **79**, 1130 (1997).
[10] A. Berger *et al.,* Phys. Rev. Lett. **85**, 4176 (2000).
[11] C. Vettier *et al.,* Phys. Rev. Lett. **56**, 757 (1986).
[12] J. F. MacKay *et al.,* Phys. Rev. Lett. **77**, 3925 (1996).
[13] N. Ishimatsu *et al.,* Phys. Rev. B **60**, 9596 (1999).
[14] J. F. Ankner and G. P. Felcher, J. Magn. Magn. Mater. **200**, 741 (1999).
[15] J. P. Hannon *et al.,* Phys. Rev. Lett. **61**, 1245 (1988).
[16] J. Stöhr, J. Magn. Magn. Mater. **200**, 470 (1999).
[17] H. Tang *et al.,* Phys. Rev. Lett. **71**, 444 (1993).
[18] J. C. Lang and G. Srajer, Rev. Sci. Instrum. **66**, 1540 (1995).
[19] S. K. Sinha *et al.,* Phys. Rev. B **38**, 2297 (1988).
[20] R. M. Osgood III *et al.,* J. Magn. Magn. Mater. **198-199**, 698 (1999).
[21] C. S. Nelson, Ph.D. thesis, Northwestern University, 1999.
[22] M. Blume and D. Gibbs, Phys. Rev. B **37**, 1779 (1988).
[23] For a given q_z, absorption modifies the scattering amplitude of layer j by $\exp[-\sum_{n=2}^{j} \mu_n (z_n - z_{n-1})/\sin\theta]$ while the phase difference between the i and j interfaces is $\exp[(ik/\sin\theta)(2\cos^2\theta(z_j - z_i) - \sum_{n=i+1}^{j} 2t_n(1 - \delta_n))]$. z_n and t_n are the average height and thickness of the interface and layer n ($z_1 = 0$ is the vacuum/cap interface and $t_1 \equiv 0$). δ_n and β_n are real and imaginary corrections to the index of refraction n_r of layer n, $n_r = 1 - \delta - i\beta$. Also, $\mu_n = (4\pi/\lambda)\beta_n$. We used tabulated values for δ_n and β_n, except for Gd for which accurate values near the Gd L_2 edge were determined from absorption measurements on the multilayer (and the related Kramers-Kronig transform).
[24] L. G. Parratt, Phys. Rev. **95**, 359 (1954); L. Nevot and P. Croce, Rev. Phys. Appl. **15**, 761 (1980).
[25] R. E. Camley, Phys. Rev. B **39**, 12 316 (1989).
[26] C. S. Nelson *et al.,* Phys. Rev. B **60**, 12 234 (1999).
[27] M. Taborelli *et al.,* Phys. Rev. Lett. **56**, 2869 (1986).
[28] P. Grunberg, Phys. Today **54**, No. 5, 31 (2001).
[29] P. Carra *et al.,* Phys. Rev. Lett. **70**, 694 (1993).
[30] J. C. Lang *et al.,* Phys. Rev. B **49**, 5993 (1994).
[31] P. A. Lindgard, B. N. Harmon, and A. J. Freeman, Phys. Rev. Lett. **35**, 383 (1975); S. Rex *et al.,* J. Magn. Magn. Mater. **192**, 529 (1999).